Modeling woody vegetation resources using Landsat TM imagery in Northern Namibia.

Authors: Alex Verlinden [a,b,c] and Risto Laamanen [b,d]

[a] Desert Research Foundation of Namibia, P.O. Box 20232 Windhoek, Namibia

[b] Directorate of Forestry, National Remote Sensing Center, National Forest Inventory, Namibia-Finland Forestry Program, P.O. Box 23930 Windhoek Namibia

[c] Institute of Nature Conservation, Kliniekstraat 25, B 1070 Brussels, Belgium

[d] Metsähallitus, P.O. Box 94 01301 Vantaa, Finland

Corresponding Author: Alex Verlinden

alexv@drfn.org.na

SUBMITTED TO REMOTE SENSING OF THE ENVIRONMENT, IN REVISION

Abstract

In 1995 a forest inventory covering Northern Namibia was initiated based on stratified systematic field sampling of plots with a radius of up to 30 m. In these plots detailed tree parameters were measured. Due to security problems the most important wooded parts of the area could not be covered completely, while the inventory method used was also very costly. This study investigated whether Landsat TM imagery could be used to estimate woody vegetation parameters as an alternative. As the existing field sampling method did not result in significant relationships between pixel values of different bands and tree cover, two sampling methods of different design were tested. Both resulted in statistically significant correlations between tree cover and pixel values of band 4 of Landsat TM. The increased size of the sample plots in both methods was the main reason for improved correlations. The relation between tree cover and Landsat TM band 4 was influenced by fire scars and patches of heavy grazing, making monitoring tree cover with satellite imagery complicated. Regression models were used to estimate cover and volumes from Landsat TM images. Estimated tree cover and volumes obtained by remote sensing were compared with volume estimates obtained by field measurements in three areas of Northern Namibia. All fell within 95 % confidence limits of the field measurements. The results suggest that Landsat TM imagery is suitable for estimating tree cover, volumes and biomass on a regional scale for dry semi-deciduous Kalahari woodland vegetation.

Keywords: Remote sensing, Landsat TM, forestry, Namibia, tree cover, tree biomass, tree volume, Kalahari woodland

Introduction

A woody vegetation inventory based upon detailed field sampling of tree parameters was started in 1995 in Namibia to obtain cover, basal density and volume estimates at species level for various regions of a total size of close to 17 million ha of mainly communal areas in northern Namibia (Chakanga et al., 1998). It was hoped that this approach would result in regional level inventories useful for strategic planning of forest resources (Erkkilä and Siiskonen, 1990). Proposals ~~Suggestions~~ were also made to use the methodology for monitoring woody resources on a long-term basis (Angombe et al., 2000). Processes of deforestation and bush thickening are important in Namibia (Erkkilä and Siiskonen, 1990; Tokola et al., 1999; Erkkilä and Löfman, 1999) and throughout southern Africa (Archer, 1995; Hudak and Wessman, 1998; Hudak, 1999; Hudak and Wessman, 2001), indicating the importance of being able to assess woody vegetation parameters on a large scale in Namibia.

Due to sporadic guerilla warfare on the Namibia-Angolan border flaring up in the late 1990s, the most important wooded parts of the area could not be covered completely, while the inventory method used was time-consuming and with costs of around 0.2 US \$ ha^{-1} causing sustainability concerns in this developing country (Verlinden and Laamanen, 2001). Remote sensing is often considered more cost-effective, reducing the amount of fieldwork, and ~~while~~ it certainly is an attractive alternative to intensive fieldwork in war zones.

This paper investigates to what extent Landsat TM imagery could be used to 1) model woody resources in areas not yet covered using limited extra field data, 2) reduce the inventory costs, and 3) monitor changes in woody resources over time. An additional requirement was that the developed method should be appropriate for a developing country with limited resources.

It has often been demonstrated that woody cover has a higher correlation with satellite imagery than other parameters such as basal area and volume (McCloy and Hall, 1991; Duncan et al., 1993; Hudak and Wessman, 2001). Previous work using remote sensing for forest cover in northern Namibia is limited, although Tokola et al. (1999) worked on calibrating Landsat TM images in northern Namibia for forest cover change detection, Erkkilä and Löfman (1999) used Landsat TM and aerial photography for forest cover change and Erkillä (2001) did a change analysis of forest cover with Landsat TM and MSS using supervised classification in a portion of northern Namibia. Forest cover change in all these studies was analyzed by comparing forested areas with non-forested areas. The present study investigates the use of Landsat TM imagery for estimating tree cover, volume and biomass on a pixel by pixel basis. This would potentially enable ~~to~~ detecting ~~detect~~ changes within forests, in addition to estimating woody resources at regional level.

Initially tests were conducted using results of the original inventory method, based on plots of maximum 30 m radius. This gave low correlations between TM waveband pixel values and various woody plant parameters (Verlinden and Laamanen, 2001).

Therefore it was decided to change the field sampling method by 1) increasing the size of the area covered in each sample and 2) ~~to compare~~ comparing the use of estimates of tree parameters with appropriate tools for a developing country with the use of more time-consuming measurements.

Material and Methods

Study Area

The area is located in ~~N~~northern Namibia, between 14 deg E and 23 deg E and 17.2 S and 19 S (Figure 1). The rainfall gradient is substantial: average 710 mm in the ~~E~~east and 350 mm in the ~~W~~west. In the ~~West~~ west, the area is characterized by *Colophospermum mopane* Kirk. ex J. Leonard shrubland and in the ~~E~~east by open woodland with *Pterocarpus angolensis* DC., *Baikiaea africana* Harms., *Guibourtia coleosperma* (Benth.) J. Leonard and *Burkea africana* Hook. This vegetation type is often referred to as dry deciduous Kalahari woodland and occurs also in adjacent areas of Angola, Botswana, Zambia and Zimbabwe. Extensive stands of *Colophospermum mopane* Kirk. ex J. Leonard trees occur also in large floodplain areas in the ~~E~~east.

The two areas where new sampling methodologies were tested are presented in Figure 1. To test the validity of the relationships between cover and pixel values of Landsat TM band 4, 27 independent samples were collected in three different regions (independent sampling areas in Figure 1) in areas considered secure from warfare at the time. Three field sampling areas where traditional field inventories were carried out were used to compare the volume estimates obtained by field measurements and satellite imagery (Figure 1).

The wide distribution of test sites in the study area ensured that the obtained results would be valid in Northern Namibia and areas with similar vegetation in adjacent countries.

Field sampling methods

Throughout the sampling, woody vegetation with diameter at breast height (1.3 m) (dbh) larger or equal than 5 cm was classified as trees. If dbh was smaller than 5 cm, the woody vegetation was classified as shrubs. Diameters were measured with calipers. Other parameters measured on trees were height and crown diameter, both with a Vertex hypsometer.

Inventory method 1

In order to test the hypothesis that a small plot size of maximum 30 m influenced the low correlations with the satellite imagery, 49 sites were visited as a part of a reconnaissance survey prior to a timber inventory in a pilot area. In each site, a tract with three sides at right angles of 100 m length was used (Figure 2). Along the tract, a recording point was laid after every 20 m. At each recording point (a total of 15 points per tract) the woody vegetation cover was estimated separately for woody plants between 2 and 4 m height and for trees taller than 4 m. A densiometer (Lemmon, 1957) was used for estimating the canopy cover in the two classes. Four readings per recording point of both height classes were taken. In addition, woody plants lower than 2 m were estimated with a Bitterlich relascope (Friedel and Chewings, 1988) sweep with factor 5 multiplier to obtain percentage canopy cover in each recording point. Average values of cover for the three woody plant classes were calculated and used in the analysis.

Inventory method 2

Using the data collected with method 1 and visual interpretation of a 3,4 and 5 band combination of a Landsat TM image, some large open areas were delineated and left out of the sampling for the timber survey in the pilot area. A systematic selection of sample units was carried out. Every 12th sampling unit (or cluster) was established in the field with a new design (Figure 2). A cluster of five plots each with a radius of 20 m was used to cover a larger area. On each plot, trees with a dbh >= 5 cm were measured (species, location, canopy diameter). The location of each tree from the central coordinate was obtained by taking the bearing with a compass and measuring the distance from the center to the tree with a Vertex distance measurer. The canopy diameter measurements in two directions were done for each tree separately without taking into account the possible overlap of adjoining crowns. Therefore the crown cover percentage of a plot includes a certain amount of overlap in dense stands. This overlap was measured in a GIS by plotting all measured trees with their canopy diameters. This allowed investigating the influence of canopy overlap on the relationships between cover and other tree parameters. Canopy overlap is defined as the difference between the measured crown cover and the projected canopy cover in each cluster.

Inside each plot, five recording points for estimating cover with the densiometer and the Bitterlich relascope were selected. Tree cover of trees with a dbh >= 0.05 m was estimated with the densiometer (four readings at each point). Woody plant cover with a dbh < 0.05 m was estimated with the Bitterlich relascope. This method allows the comparison of results obtained by measuring tree canopy parameters with results obtained by estimating these with the densiometer and the Bitterlich relascope used in method 1. Using the densiometer is a much faster method to estimate canopy cover than measuring individual tree crown cover and therefore this method was tried to see if it could replace the time-consuming measurements.

Volume and biomass estimates

A total of 247 trees of 7 species in four areas were felled for volume and biomass functions. Figure 3 shows the diameter distributions of the felled trees, demonstrating that a wide range of diameters was used for the calculations. Two volume functions were derived and all tree species were allocated to one of the two models and to one of the 7 reference species (NFI, 1997, Chakanga et al. 1998):

1) $\ln(v) = a0 + a1*d + a2*d^2$

2) $v/d^2 = (a0 + a1*d + a2*d^2)$

where v= volume (dm^3)

d= diameter at breast height (cm)

Table 1 lists the 7 reference species with their volume function parameters and volume functions used in the calculations. Table 2 lists all species in the inventories with their reference species for the volume calculations.

The same trees used for volume estimates were also used for estimating biomass conversion factors by dry-weighing the tree samples (NFI, 1997). Volume and biomass was calculated for all the samples collected with inventory method 2.

Remote Sensing

A total of twelve images (Enhanced Thematic Mapper ETM+ and TM 5) were examined (Table 3). For one of the TM5 scenes only bands 1, 2, 3 and 4 were purchased, the others had the full waveband range.

All satellite images were selected primarily on having cloud-free data and on the same seasonal phase of the vegetation. The end of the wet season and the early dry season (April-May) are in Northern Namibia considered to be the optimal period for detecting woody plant vegetation (Erkkilä and Löfman, 1999; Tokola et al., 1999).

All images used in the analysis had already been rectified by the supplier but had to be re-registered with co-ordinates obtained by GPS in the survey areas during field trips.

Only GPS data of 2001 and 2002 were used, as previous data were less accurate. Registration used in the analysis reduced geometrical errors to a Root Mean Square Error (RMSE) of less than 30 m. Overlays with GPS tracks and points collected during field trips in three of the study areas confirmed position errors of less than 30 m between satellite image registration and GPS locations. This does however not ensure that the pixel exactly corresponding with the central location of the field sample is used in analysis of the first sampling method, as the nearest neighbor re-sampling method was used in registration of the images. This method ensures that the original pixel values are retained.

To estimate cover across several images, pixel values had to be transformed as histograms of each scene are different. Histogram matching of band 4 was used with the algorithm provided in ER Mapper software (ER Mapper2002) to match the output histogram to the histogram of a reference image. The scene of Path 177 and Row 073 of 24 April 2000 was used as reference as it covered the largest sampling area. During
mosaicked (British spelling)
histogram matching, the scenes were mosaiced to form one single band scene covering the whole study area. Histogram matching was chosen as it was the easiest technique for a local team to adopt the methodology as other calibration methods are complicated and did not result in very high accuracy in northern Namibia (Tokola et al. 1999).

An accuracy analysis of the method was carried out with random sampling of pixels in overlapping areas of 2 images adjacent to the reference images. Boolean images with randomly located sample points were prepared of the overlapping areas. These images were used to extract the corresponding pixel values of the reference image and the adjacent histogram matched images. Linear regression analysis was then used to assess the accuracy of the matched areas.

To extract pixels for exploring relationships with TM bands and woody plant cover in method 1 (Figure 2), a square of 100 x 100m with the starting GPS coordinate on one corner of the square sample was drawn in IDRISI GIS package (Eastman, 2000). This area represents the area covered by each sample in the field. The resulting polygons were converted to a Boolean raster image with exactly the same registration as the Landsat TM image mosaic. This Boolean image was used to extract the pixel values of the different bands of the satellite image mosaic that fell within the 100 x 100 m square. The average value of all pixel values with more than 50% of their areas falling within the 100x100m square was calculated with IDRISI and used for statistical analysis.

For method 2 (Figure 2), circular buffers with a 100m radius around the GPS coordinates of the central position of each sample were drawn. The resulting polygons were imported into IDRISI and converted to a Boolean raster image with the same registration as the corresponding Landsat TM image mosaic. This Boolean image was used to extract the pixel values of the different bands of the satellite image mosaic that fell within the 100 m radius. The average value of all pixel values with more than 50% of their areas falling within a 100 m radius of the central location of the sample was used for the statistical analysis. This ensures that the majority of the pixel values corresponding with the areas covered by the field samples are represented in the analysis.

For the analysis bands 1, 2, 3, 4, 5, 7 were used, while also the Normalized Vegetation Index (NDVI) was calculated.. NDVI is often used as it has been demonstrated in many cases to be correlated to green biomass in semi arid areas (Tucker, 1979; Danaher et al. 1992; Duncan et al., 1993; Verlinden and Masogo 1997), although Ringrose et al. (1994) found that green vegetation exhibited varying response curves in different climatic zones across all Landsat MSS wavebands and NDVI is therefore not always reliable.

Statistical analysis of the data

As not much is known about relationships between woody plant parameters and remote sensing in the study area, several models were tested for the relationships between woody cover and pixel values of individual bands. For modeling woody parameters basal area, biomass and volume based on crown cover, various commonly used regression models in forestry were used.

Modeling of woody parameters

To meet requirements of forest inventory and woody resource monitoring, cover data need to be significantly correlated to basal area and volume. Regression analysis was used to test these requirements. Possible influences limiting high correlations between cover and stand basal area are: canopy diameter overlap resulting in differences between calculated crown cover and canopy cover, and the errors involved in using densiometers to estimate canopy cover instead of measuring canopies. These possible influences were explored to estimate their importance.

The data of 312 plots was used to examine the relationship between basal area of trees and crown cover percentage (Figure 4). Two outlier observations (plots) were removed because of errors in the data recording in the field.

Testing a linear model gave the following results:

Predicted Basal Area (m^2ha^{-1}) = -0.05476 + 0.1884 Calculated crown cover (%) r^2_{adj} = 0.66, R =0.83, SE= 1.68, F= 595, $p<0.001$, N=312

Very often biomass data are required for monitoring programs. These can be obtained using the following equation (Figure 4):

Biomass (air dry tons ha^{-1}) = 4.1179 + 1.1325*cover% r^2_{adj}= 0.64 (R = 0.80) SE = 12.7 F = 555.2, $p < 0.001$, N = 312

Volume here means the volume of the whole trees including branches per hectare. In order to be able to compare traditional inventory results with cover estimates from satellite imagery, a relationship between mean volume estimates (in m^3 ha^{-1}) and tree cover percent data had to be derived. Using the plot data from the three areas where field data ~~has been~~ was collected using method 2 the following regression equation was obtained (Figure 4):

Tree volume (m^3 ha^{-1}) = 5.261 + 1.394*cover%, r^2_{adj} = 0.62 (R = 0.77), SE = 16.5, F = 501.998, $p < 0.001$, N=312

Evaluation of Models

A raster-based GIS was used to calculate average cover for certain areas and corrected for canopy overlap to derive average volumes in m^3 ha^{-1} for three test areas where detailed forest inventory data were collected. The following three sites form the independent test data available to evaluate the results obtained by the method developed here using satellite imagery (Figure 1):

- Caprivi Region (old boundary demarcation)
- Caprivi State Forest
- Okongo Community Forest

Finally, average tree cover and volumes were calculated for areas where no field data were collected due to security problems.

Results

Accuracy of histogram matching

Linear regression analysis of 654 random samples between pixel values of the reference image and adjacent overlapping images where were histogram matching was applied is presented in Figure 5. The Pearson correlation coefficient between reference image and matched images was R= 0.85 with an adjusted coefficient of determination r^2_{adj}= 0.73.

Correlations between satellite data and canopy cover

Pearson correlation coefficients between total tree cover, shrub cover estimated with method 1, and pixel values of the individual bands are presented in Table 4. The highest correlations were found in the near infrared waveband, TM band 4. Both trees and shrubs are significantly correlated, but tree cover decreases with increasing pixel values of TM waveband 4 while shrub cover increases with TM waveband 4.

Pearson correlation coefficients between measured (method 2) total tree cover, shrub cover and pixel values of the individual bands are presented in Table 5. Again the highest correlations are found with TM waveband 4 but they are slightly higher than with method 1.

Vegetation cover models

As Table 4 and 5 illustrate that correlations between methods 1 and 2 are similar and the data are not significantly different from each other, samples were pooled to calculate regression equations for tree and shrub cover with pixel values of band 4.

For trees the resulting model is:

Tree cover % = 126.99 – 1.166 band 4 (r^2_{adj}= 0.51, r = 0.72, F_{64} = 55.8, P <0.001)

For shrubs the resulting model is:

Shrub cover% = -54.79 + 0.115 band 4 (r^2_{adj}=0.48, r = 0.69, F_{64} = 43.5 P <0.001)

This negative relationship between trees and shrubs in a relatively dense woodland area suggests that reflectance of the overstory may override reflectance of the understory and that the equation for shrubs is an artifact.

It appeared that several outliers suggested two different relations between tree cover and pixel values of band 4. Upon closer inspection of the images it appeared that in most sandy soils fire scars of the previous dry season could still be observed and they appeared to have an influence on the relationship. Areas not affected by fire scars or by heavy grazing the subsequent wet season show a lower canopy cover with the same pixel values as compared with the affected areas. This relationship is demonstrated in Figure 6. It appeared that the majority of samples belonging to the affected areas are in the dry deciduous Kalahari woodlands.

For not affected areas the resulting model is:

Tree cover = 147.5 – 1.560 Band 4 (r^2_{adj} = 0.52, r = 0.75, SE estimation =7.2, F = 16.4, p<0.0001)

For fire and grazing affected areas the resulting model is:

Tree cover = 141.337 – 1.298 Band 4 (r^2_{adj} = 0.59, r=0.77, SE estimation = 8.04, F= 66.4, p<0.0001)

27 independent samples collected in 2002 in two different areas of Kavango (one in the West, one in the East) and one area in East Caprivi were used to test the accuracy of regression equations obtained. The areas in Kavango were sampled with method 2, the one in East Caprivi with method 1. For affected areas the coefficient of determination between the predicted and calculated tree cover was r^2_{adj}= 0.7 (correlation R=0.85). For the not affected areas the correlation between the predicted and calculated tree cover was r^2_{adj}=0.67 (R=0.83). The overall coefficient of determination between the predicted tree cover and calculated cover in the field was r^2_{adj}=0.77 (R=0.88). There is ~~a~~ good agreement between estimated and observed values, especially taking into account that 1) there is a distance of more than 500 km between samples, 2) there is a big difference between vegetation types (Kalahari woodland and *Colophospermum mopane* woodlands), 3) there is a time difference between tree measurements and the image and 4) there are possible image processing errors (image registration, histogram matching). The relationship between the estimated and measured tree cover is shown in Figure 7. The graph shows that at high calculated crown cover the estimated tree cover from the regression equations is an underestimate. Because of overlapping canopies, the calculated cover percentage includes a certain overlap. This overlap was analyzed with a GIS by plotting the tree crowns in 36

clusters on their exact locations and defining the projected coverage. The overlaps on each cluster are shown in Figure 8 and the 2nd order polynomial has a coefficient of determination of $r^2_{adj} = 0.90$ with the calculated crown coverage.

The overlap is fairly low – less than 2 %-units – up to a measured cover of 20 %. With higher covers, the overlap increases rapidly. This suggests that at higher cover levels, canopy cover might be significantly underestimated with remote sensing when the calculated crown cover percentage is used without correction for overlap. The influence of canopy overlap largely explains the underestimate at high cover observed in Figure 7.

Densiometer readings and canopy measurements were obtained on 64 clusters (Figure 9). In principle, the densiometer estimates should be lower as there is no crown overlap in the readings. However, the figure shows that the densiometer in many cases gives an overestimate. In measured woody plant data, shrubs were defined to have a dbh less than 5 cm. However, the height of a shrub can be 4 meter or more and there is a risk of including them in the densiometer counting. This has been corrected in subsequent measurements in the field. The coefficient of determination r^2_{adj} between densiometer readings and calculated crown cover is 0.67.

Evaluation of models

For results of the estimated volumes using remote sensing to be accurate, estimates should fall within the calculated 95 % confidence limits of the averages obtained by field inventories. Table 6 demonstrates that most estimates are somewhat below average, but all estimates fall within the 95 % confidence limits.

Table 7 summarizes results of the average volumes per hectare obtained from the estimated average tree cover derived from remote sensing data for regions and areas that were not yet covered by the field based inventory method. It has to be noted that the method presented here has the additional advantage that new estimates can quickly be calculated when boundaries of regions change as happened in 2000 with the boundaries of Caprivi and Kavango regions.

Discussion

Size of plots has an influence on correlation between tree and shrub cover and TM wavebands. Plots with a maximum radius of 30 m are not necessarily representative ~~for~~ of the immediate surroundings, while positioning errors with the GPS before 2000 and errors of satellite image registration possibly contribute to low correlations. Small size of plots ~~was~~ is apparently more influential for trees than shrubs, as correlations between shrub cover and TM wavebands ~~were~~ are higher (Verlinden and Laamanen, 2001).

The image calibration with histogram matching gave satisfactory results, although the correlation of R= 0.85 and the scatter around the regression line showed that errors of up to 5 % tree cover on a pixel basis as result of the calibration method are to be expected.

A negative relationship between tree cover and shrub cover in the more wooded vegetation types characterized by *Burkea africana*, *Baikiaea plurijuga*, *Guibourtia coleosperma* and *Pterocarpus angolensis* was demonstrated. High influence of subcanopy when the overstory has a low cover has been found elsewhere, usually with high reflectance in the NIR as opposed to stands with a high cover of the overstory (Butera, 1986).

Different models obtained for trees and shrubs suggest that total woody vegetation cover is in ~~the~~ northern Namibian conditions not a useful parameter to monitor by ~~with~~ remote sensing and that different woody layers have to be treated separately. It has been shown that increased shadows and dark background decrease reflectance (Koch et al., 1990). Shadows are likely to influence imagery in this study as images are captured early in the morning before 9 am. Moleele et al. (1999) found significant correlations of a shrub layer between 0.3 – 1.5 m and mid infrared Landsat TM bands 5 and 7. This suggests that different models need to be tested for shrub dominated vegetation types in Namibia.

There were no significant differences between the results of inventory methods 1 and 2 of this study, although method 2, based on measurements of woody plants, performed slightly better than method 1, based on estimated woody plant parameters. This means that densiometers and Bitterlich relascopes are cost-effective in woodland types where already sufficient measurements have been acquired to test validity of established models between vegetation cover, biomass and volumes.

The observed influence of fire and heavy grazing complicates not only the estimate of woody cover as additional data are required to distinguish between affected and unaffected areas, but also monitoring woody cover change. It appear~~ed~~s that fire or grazing ~~did~~ does not affect floodplain areas and areas with *Colophospermum mopane* the subsequent season. It is mainly sandy soils with Kalahari woodland that show the observed effect of increased reflectance in the NIR. Colwell (1974) found that an increase in reflectance in NIR occurs when the background is bright, such as grass or light colored soils. Most Kalahari sandy soils in the study area are light in color. In view of the low number of samples in Kalahari woodland that were not affected by fires or heavy grazing or a light background soil color, one can apply the equation of affected areas on the whole area covered by this vegetation type and still fall within the 95% confidence limits of inventory results. Interference by fire was also observed by Danaher et al. (1998). This interference means one has to be very prudent with change detection results using a limited number of images in a time series. The results of this study suggest that monitoring woody cover should use several images in conjunction with fire scar maps to be able to interpret changes, but more research is needed to evaluate the use of the methodology for monitoring woody cover change. This study suggests that with errors due to fire impact, histogram matching and errors in tree cover estimates, only changes of more than 30 % canopy cover should be considered significant in change analysis.

That TM band 4 was shown to be the most useful band for modeling tree cover is not unique although in the NIR region, the correlation between volume and volume related variables versus reflectance may vary from positive (Spanner et al., 1990) ~~over~~ To, no no correlation (Franklin, 1986) to negative (Poso et al., 1987).

Khorram et al. (1990) regressed % defoliation on TM band 4 with altitude and elevation as independent variables and found high coefficients of determination, partly a result of adding elevation. The latter is unnecessary as the present study area is very flat.

The validity test of regression equations with a different dataset indicated that the equations are valid for a very large area and for the two main woodland vegetation types in northern Namibia and surrounding areas. It also demonstrates that the method of calibration of the images using histogram matching is acceptable across different scenes and woodland types with this calibration method.

This study confirmed correlations between tree cover, basal area, biomass and volumes found elsewhere (Butera, 1986; Kleman, 1986; Poso et al., 1987; Brockhaus and Korram, 1989; Koch et al., 1990). Comparison between volume estimates obtained by traditional inventory methods and with estimates obtained with the remote sensing derived method indicates that there is an overall good agreement. Estimates using remote sensing derived equations all fell within the 95 % confidence limits of the forest inventory data. Especially when the regions were very large, estimates were close to the average obtained by field inventories. For areas with a relatively high volume per hectare, estimates are below average. Although the woodlands in the study area are open, it is possible that at higher canopy cover levels of over 30%, the low reflectance in NIR underestimates cover due to more shadows (Ekstrand, 1993).

While the traditional inventory method gives an indication of species composition but limited indication of spatial distribution, the method developed here gives detailed high resolution distribution information but no information on species composition. It can be argued that there are faster methods to get reliable information on species composition and frequencies than an inventory, or information on frequencies from inventories located nearby can be used.

Landsat TM imagery is available at approximately 0.0002 US $ per ha. Taking into account the limited processing needed for calculating cover and deriving volumes, it is suggested that Landsat TM imagery is a cost-effective alternative to field sample-based inventories for regional woody resources assessment with respect to total tree cover, volumes, basal area and biomass for similar woodland types in Angola, Zambia, Zimbabwe and Botswana. Future inventory designs in developing countries should take into account the requirement of large-sized plots to be able to use the data in remote sensing.

Acknowledgements

The authors thank the inventory staff of the Directorate of Forestry under the guidance of Simon Angombe and Ndapanda Kanime for assistance in the data collection. This work was supported by Lux-Development S.A. (Agence Luxembourgeoise pour la Coôperation au Développement) and DCIC (Department for International Cooperation, Finland).

References

Angombe, S. Selanniemi, T. & Chakanga, M. (2000). Inventory Report on the woody Resources in the Okongo Community forest. Ministry of Environment and Tourism, Namibia Finland Forestry Program, National Forest Inventory Program, 56 pp.+ Appendices

Archer, S. (1995). Tree-grass dynamics in a Prosopis-thornscrub savanna parkland: reconstructing the past and predicting the future. *Ecoscience, 2*, 83-99

Brockhaus, J.A., & Khorram, S. (1992). A comparison of SPOT and Landsat TM data for use in conducting inventories of forest resources. *International Journal of Remote Sensing*, *13*, 3035-3043

Butera, M.K. (1986). A correlation and regression analysis of percent canopy closure versus TMS spectral response for selected forest sites in the San Juan National Forest, Colorado. *IEEE Transaction on Geoscience and remote sensing, 24*, 122-129

Chakanga, M., Korhonen, K. & Selanniemi, T. (1998). Forest inventory report of Caprivi Region. Ministry of Environment and Tourism. Namibia Finland Forestry Program, Windhoek Namibia, 45pp.

Colwell, J.E. (1974). Vegetation canopy reflectance. *Remote Sensing of Environment, 3*, 175-183

Danaher, T.J., Carter, J.O., Brook, K.D., Peacock, A. & Dudgeon, G.S. (1992). Broad-scale vegetation mapping using NOAA-AVHRR imagery. (pp. 128-137). *Sixth Australasian Remote Sensing Conference Proceedings,* Remote Sensing and Photogrammetry Association of Australia,

Danaher, T.J., Bishop, G., Kastanis, L. & Carter, J.O. (1998). The Statewide Landcover and Trees Study (SLATS) – Monitoring Land cover change and greenhouse gas emissions in Queensland. *Ninth Australasian Remote Sensing Conference Proceedings, Sydney, Australia, 3*, 16-28

Duncan, J., Stow, D, Franklin, J. & Hope, A. (1993). Assessing the relationship between spectral vegetation indices and shrub cover in the Jornada Basin, New Mexico. *International Journal of Remote Sensing, 14*, 3395-3416

Eastman, J.R. (2000). *IDRISI, Guide to GIS and image processing.* (pp. 1-350). Worcester, MA., Clark University

Ekstrand, S. (1993). Assessment of forest damage using Landsat TM, elevation models and digital forest maps. Ph.D. thesis, (pp. 1-110). Stockholm, Sweden, Royal Institute of Technology

ER Mapper (2002). Earth Resource Mapping software. Earth Resource Mapping, Pty., Perth, Australia

Erkkilä, A. (2001). Living on the land: change in forest cover in north-central Namibia 1943-1996. *Silva Carelica, 37*, 1-118

Erkkilä, A. & Siiskonen, H. (1992). Forestry in Namibia 1850-1990. *Silva Carelica, 20*, 1–245

Erkkilä. A. & Löfman, S. (1999). Forest cover change in the Ohangwena region, northern Namibia: a case study based on multitemporal Landsat images and aerial photography. *South African Forestry Journal, 184*, 25-32

Franklin, J. (1986). Thematic Mapper analysis of coniferous forest structure and composition. *International Journal of Remote Sensing, 7*, 1287-1301

Friedel, M.H. & Chewings, V.H. (1988). Comparison of crown cover estimates for woody vegetation in arid rangelands. *Australian Journal of Ecology, 13*, 463-468

Hudak, A.T. and Wessman, C.A. (1998). Textural analysis of historical aerial photography to characterize woody plant encroachment in South African savanna. *Remote Sensing of Environment, 66*, 317-330

Hudak A.T. & Wessman, C.A. (2001). Textural analysis of high resolution imagery to quantify bush encroachment in Madikwe Game Reserve, South Africa, 1955-1996. *International Journal of Remote Sensing, 22*, 2731-2740

Hudak, A.T. (1999). Rangeland mismanagement in South Africa: failure to apply ecological knowledge. *Human Ecology, 27*, 55-78

Khorram, S., Brockhaus, J.A., Bruck, R.R.I. & Campbell, M.V. (1990). Modelling and Multitemporal evaluation of forest decline with Landsat TM digital data. *IEEE Transactions on Geoscience and Remote Sensing, 28*, 746-748

Koch, B., Ammer, U., Schneider, T. & Wittmeier, H. (1990). Spectroradiometer measurements in the laboratory and in the field to analyse the influence of different damage symptoms on the reflection spectra of forest trees. *International Journal of Remote Sensing, 11*, 1145-1163

Lemmon, P. (1957). A new instrument for measuring forest overstory density. *Journal of Forestry, 55*, 667-668

McCloy, K.R. & Hall, K.A. (1991). Mapping the density of woody vegetative cover using Landsat MSS digital data. *International Journal of Remote Sensing, 11*, 2035-2049

Moleele, K., Ringrose, S., Arnberg, W., Lunden, B. & Vanderpost, C. (1999). Estimation of potential browse biomass using Thematic Mapper derived indexes and transforms from a bush encroached area in semi-arid Botswana. In: Moleele, K. (Ed.) Bush encroachment and the role of browse in cattle production. The Department of Physical geography, Stockholm University, *Dissertation series, 13*, 1-16

NFI (1997). Field instructions: Collection of sample tree data for biomass and volume tables. National Forest Inventory Project. Ministry of Environment and Tourism, Directorate of Forestry, Namibia Finland Forestry program, Windhoek, Namibia, 37pp.

Poso, S., Paananen, R. & Similä, M (1987). Forest inventory by compartments using satellite imagery. *Silva Fennica, 21*, 69-94

Ringrose, S., Matheson, W., Matlala, C.J.S.S. & O'Neill, T. (1994). Vegetation spectral reflectance along a north-south gradient in Northern Australia. *Journal of Biogeography, 21*, 33-47

Spanner, M.A., Pierce, L.L., Peterson, D.L. & Running, S.W. (1990). Remote sensing of temperate coniferous forest leaf area index. The influence of canopy closure, understory vegetation and background reflectance. *International Journal of Remote Sensing, 11*, 95-111

Tokola, T., Löfman, S. & Erkkilä, A. (1999). Relative calibration of multitemporal Landsat data for forest cover change detection. *Remote Sensing of Environment*, *68*, 1-11

Trotter, C.M., Dymond, J.R. & Goulding, C.J. (1997). Estimation of timber volume in a coniferous plantation forest using Landsat TM. *International Journal of Remote Sensing, 18*, 2209-2223

Tucker, C.J. (1979). Red and photographic infrared linear combinations for monitoring vegetation. *Remote Sensing of Environment, 8*, 127-150

Verlinden, A. & Masogo, R.M.M. (1997). Satellite remote sensing of habitat suitability for ungulates and Ostrich in the Kalahari. *Journal of Arid Environments, 35*, 563-574

Verlinden, A. & Laamanen, R. (2001). The role of remote sensing in monitoring woody resources in northern Namibia. In Lusepani-Kamwi, E & Chikasa, P. (Eds.), Proceedings of the first national forestry research workshop 12-13 March. (pp. 15-28). Windhoek, Namibia

Table 1. List of species with parameters for volume functions of 7 reference species. Volume function parameters were derived from cut trees. The last column refers to the type of volume function (f) used for the species. f(1) is $\ln(v) = a0 + a1*d + a2*d^2$ and f (2) $v/d^2 = (a0 + a1*d + a2*d^2)$

Species	a0	a1	a2	f
1. *Baikiaea plurijuga* Harms	0.2501141	0.0227406	-0.000198461	2
2. *Burkea africana* Hook.	0.0976836	0.034642	-0.000334653	2
3. *Colophospermum mopane* Kirk ex Leonard	0.12798339	0.01580639	-0.00014894	2
4. *Combretum collinum* Fresen	0.1932033	0.0199121	-0.000108192	2
5. *Lonchocarpus nelsii* Schinz ex Heering & Grimme	0.46735748	0.00342083	0.00008758	2
6. *Pterocarpus angolensis* DC.	2.7760988	0.1426546	-0.000868738	1
7. *Terminalia sericea* Burch. ex DC.	0.21795109	0.01407904	-0.00010783	2

Table 2. List of all species with family and volume model in the inventories. In column model the numbers correspond with the reference trees of table 1 used for calculating volumes.

Species	Family	model
Acacia ataxacantha DC.	Mimosoideae	1
Acacia erioloba E. Meyer	Mimosoideae	1
Acacia fleckii Schinz	Mimosoideae	1
Acacia polyacantha Willd.	Mimosoideae	7
Acacia schweinfurthii Brenan & Exell	Mimosoideae	1
Ancylanthos bainesii Oliver	Rubiaceae	7
Baikiaea plurijuga Harms	Caesalpinioideae	1
Baphia massaiensis Taub.	Papilionoideae	7
Bauhinia petersiana Bolle	Caesalpinioideae	7
Boscia albitrunca (Burch) Gilg & Benedict	Capparaceae	6
Burkea africana Hook.	Caesalpinioideae	2
Colophospermum mopane Kirk ex Leonard	Caesalpinioideae	3
Combretum apiculatum (Schinz) Exell	Combretaceae	7
Commiphora africana (a. Rich) Engl.	Burseraceaea	4
Commiphora angolensis Engl.	Burseraceaea	4
Combretum collinum Fresen.	Combretaceae	4
Combretum elaeagnoides Klotzch	Combretaceae	4
Combretum engleri Schinz	Combretaceae	4
Combretum psidioides Welw.	Combretaceae	4
Combretum zeyheri Sonder	Combretaceae	4
Croton gratissimus Burch.	Euphorbiaceaea	7
Dialium engleranum Henriques	Caesalpinioideae	7
Dichrostachys cinerea (L.) Wight & Arn.	Mimosoideae	7
Diplorhynchus condylocarpon Pichon	Apocynaceae	7
Dombeya rotundifolia (Hochst) Planchon	Sterculiaceae	7
Erythrophleum africanum (Welw. Ex Benth.) Harms	Caesalpinioideae	2
Grewia flavescens Juss.	Tiliaceae	7
Grewia bicolor Juss.	Tiliaceae	7
Grewia flava DC.	Tiliaceae	7
Grewia retinervis Burret	Tiliaceae	7
Guibourtia coleosperma (Benth.) J. Leonard	Caesalpinioideae	6
Lonchocarpus nelsii Schinz ex Heering & Grimme	Papilionoideae	5
Markhamia acuminate (Klotsch) K. Schum.	Bignoniaceae	2
Mundulea sericea (Willd.) Chev.	Papilionoideae	7
Ochna pulchra Hook.	Ochnaceae	6
Ozoroa insignis Delile	Anacardiaceae	7
Ozoroa longipes (Eng. & Gilg.) R. & A. Fernandes	Anacardiaceae	7
Ozoroa paniculosa (Sonder) R. & A. Fernandes	Anacardiaceae	7
Ozoroa schinzii	Anacardiaceae	7
Pavetta zeyheri Sonder	Rubiaceae	7
Peltophorum africanum Sonder	Caesalpinioideae	6
Pseudolachnostylis maprouneifolia Pax	Euphorbiaceae	7
Pterocarpus angolensis DC.	Papilionoideae	6
Rhigozum brevispinosum Kuntze	Bignoniaceae	7
Rhus tenuinervis Engl.	Anacardiaceae	7
Schinziophyton rautanenii	Euphorbiaceae	2
Securidaca longepedunculata Fresen	Polygalaceae	6
Steganotaenia araliacea Hochst.	Apiaceae	6
Strychnos cocculoides Baker	Loganiaceae	7

Strychnos pungens Solereder	Loganiaceae	7
Terminalia sericea Burch. ex DC.	Combretaceae	7
Vangueria infausta Burch.	Rubiaceae	6
Ximenia americana L.	Olacaceae	6
Ximenia caffra Sonder	Olacaceae	6

Table 3. The satellite imagery used in the study

Sensor	Path/Row	Date
TM5 (band1-4 only)	174/072	24 May 2000
TM5 (band1-4 only)	174/073	24 May 2000
ETM+	175/072	10 April 2000
ETM+	175/073	10 April 2000
ETM+	176/072	12 March 2000
ETM+	176/073	4 June 2000
ETM+	177/072	24 April 2000
ETM+	177/073	24 April 2000
ETM+	178/072	4 July 2000
ETM+	178/073	17 May 2000
TM5	179/072	29 April 1997
ETM+	180/072	22 April 2000

Table 4: Tree cover (T) and shrub cover (S) Pearson Correlation Coefficients (R) with average pixel values of 6 TM wavebands and NDVI in a 100 m square around the central point of the sampling area using inventory method 1 (n=49). **: Correlation is significant at the 0.01 level (2-tailed); *: Correlation is significant at the 0.05 level (2-tailed)

Type	R (b1)	R (b2)	R (b3)	R (b4)	R (b5)	R (b7)	R (NDVI)
Trees	-0.23	-0.25	-0.50**	-0.66**	-0.39*	0.25	0.14
Shrubs	-0.05	0.20	0.17	0.65**	0.27	-0.11	0.21

Table 5: Tree cover (T) and shrub cover (S) Pearson Correlation Coefficients (R) with average pixel values of 6 TM wavebands and NDVI in a 100 m radius around the central point of the sampling area using inventory method 2 (n=19). **: Correlation is significant at the 0.01 level (2-tailed); *: Correlation is significant at the 0.05 level (2-tailed)

Type	R (b1)	R (b2)	R (b3)	R (b4)	R(b5)	R(b7)	R(NDVI)
Trees	-0.28	-0.40	-0.35	-0.74**	-0.41	0.25	0.14
Shrubs	-0.04	0.17	0.11	0.70**	0.11	-0.07	0.52*

Table 6: Comparison between estimated tree volumes derived from estimated tree cover with remote sensing data and calculated tree volumes obtained by field based inventory data

Area	Cover estimate (%)	Mean volume estimate from satellite images (m^3ha^{-1})	Mean volume estimate from inventory (m^3ha^{-1})	95% confidence limits of inventory mean
Okongo	18.34	32.32	45	32 – 58
Caprivi region (old boundary)	11.12	21.26	21.37	20.25-22.49
Caprivi State Forest	16.85	29.75	33.3	28 – 37

Table 7. Cover % and mean volume estimates based on remote sensing for some regions previously not assessed or with a recent new boundary

Region	Cover estimate (%)	Volume Estimate (m3/ha)
Ohangwena	11.234	21.4
Ohangwena wooded area	13.316	24.52
Kavango (new boundary)	11.58	21.9
Kavango (old boundary)	11.63	21.97
Caprivi (new boundary)	11.14	21.3

Figure 1. The insert below shows the location of Namibia in Africa. The map below shows Namibia and neighbouring countries. The map on top shows the areas used for sampling woody plants with methods 1 and 2 and the areas used for testing the resulting models with independent samples and areas used for comparison of volume data calculated from field inventories and volumes estimated from models based on remote sensing (Caprivi, State forest and Okongo).

Figure 2. Design of the 2 alternative field inventory methods. 1: Method 1 estimates canopy cover using densiometer and Bitterlich gauge. The dots indicate where densiometer readings and Bitterlich gauge readings were done. GPS readings were taken at each corner point. 2: method 2 uses measurements of woody plant parameters in the circular plots combined with Bitterlich gauge and densiometer readings.

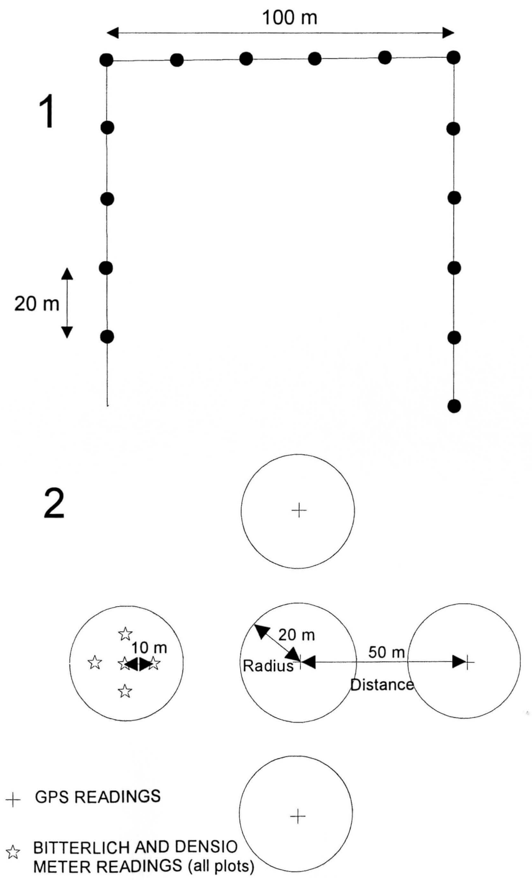

Figure 3. Diameter distributions measured at 1.3 m height of the trees felled for calculation of volume functions in Table 1. Note that the scale ~~is~~ ~~can~~ may differ between the graphs. No of obs = number of observations.

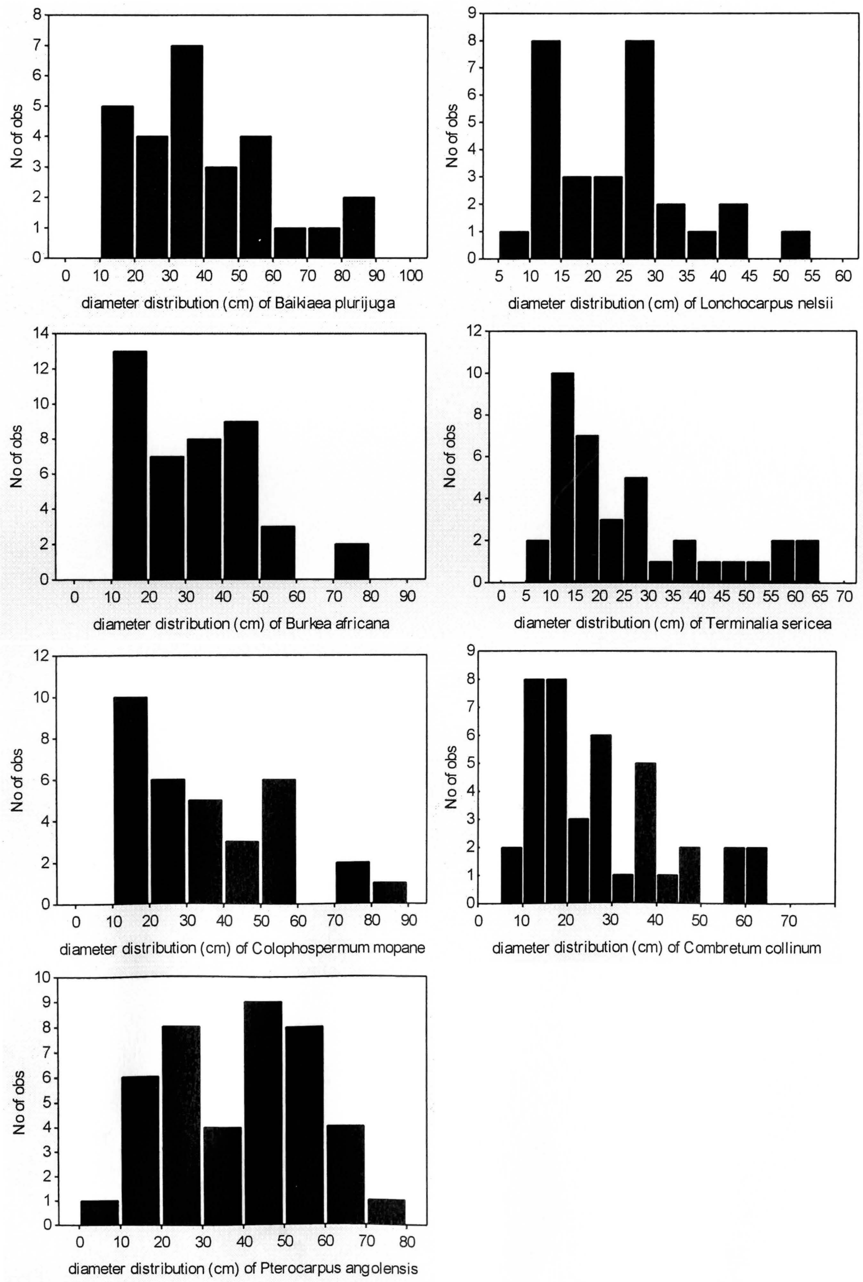

Figure 4. Relationships between basal area (m^2ha^{-1}), estimated biomass (tons ha^{-1}), volume (m^3ha^{-1}) and calculated crown cover (%). N= 312.

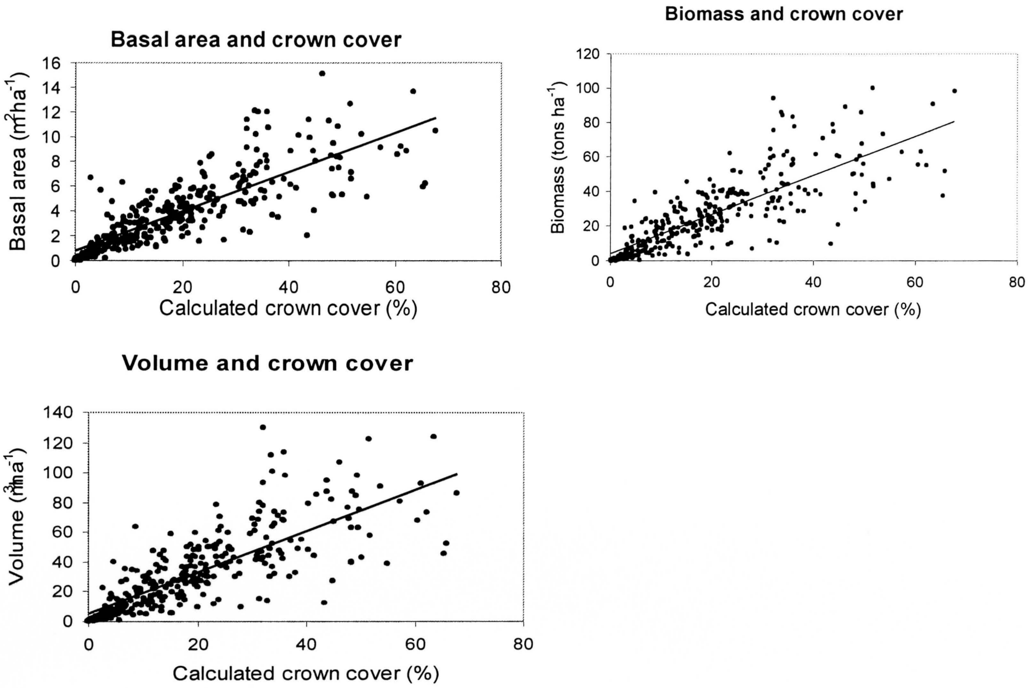

Figure 5: Frequency scatterplot with linear fit based on random sampling of pixel values of TM band 4 of the reference image and 2 histogram matched images adjacent to the reference image (r^2_{adj} =0.73, N= 654).

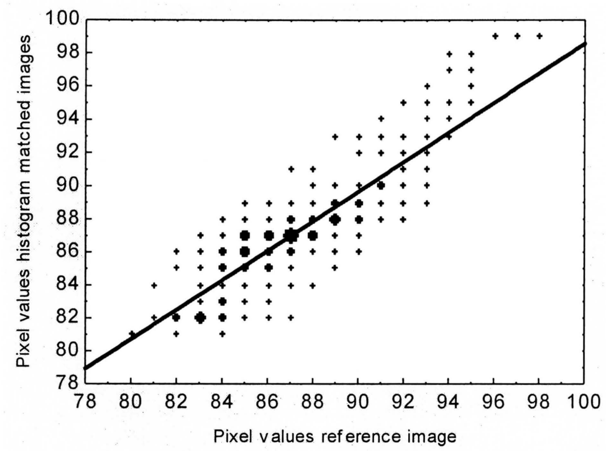

Figure 6: Regression analysis of tree cover and values of spectral waveband 4 with the distinction of areas affected or not by fire and heavy grazing. The graph shows that different maximum and minimum thresholds in the band 4 image should be applied for each equation (N = 88).

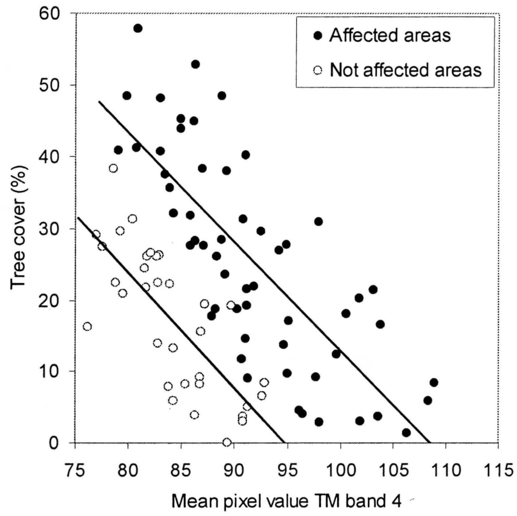

Figure 7. Relationship between measured tree cover and estimated tree cover using regression equations with an independent dataset (N = 27)

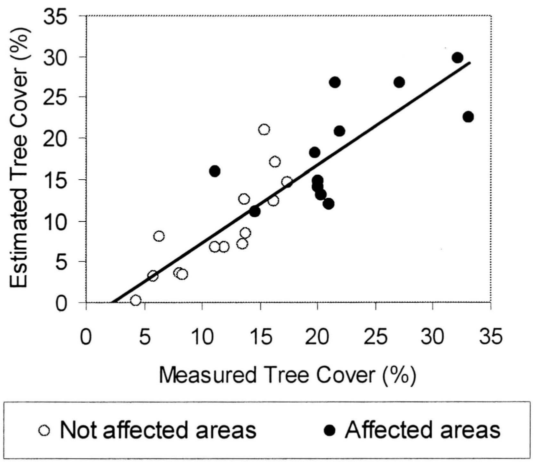

Figure 8. Relationship between canopy overlap obtained by GIS analysis of overlapping crown projections and calculated crown cover from measured crown diameters of separate trees (N=36).

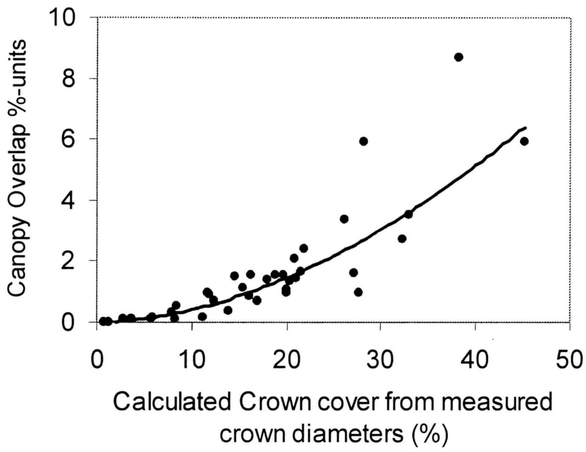

Figure 9. Relationship between crown cover measured with the densiometer and the calculated crown cover from measured crown diameters (N= 64).